

## G106.3+2.7: a candidate PeVatron with ASTRI Mini-Array

**A. Tutone<sup>a,\*</sup> and M. Cardillo<sup>b</sup> for the ASTRI Project\***

<sup>a</sup>*National Institute for Astrophysics (INAF),  
00136, Rome (RM), Italy*

<sup>b</sup>*Istituto di Astrofisica e Planetologia Spaziali (INAF),  
Via del Fosso del Cavaliere 100, 00133 Roma (RM), Italy*

*E-mail:* [antonio.tutone@inaf.it](mailto:antonio.tutone@inaf.it)

The SNR G106.3+2.7, with its associated molecular cloud complex, is one of the candidate TeV counterparts of LHAASO J2226+6057, one of the 12 sources detected by LHAASO at  $>100$  TeV. The other candidate is the Boomerang PWN, associated with the PSR J2229+6114. This VHE region has been detected by different  $\gamma$ -ray facilities. It has an elongated morphology: the SNR is located in the “tail” of the VHE emission and the PWN is in the “head”. Identifying the exact location of the emission at  $> \sim 100$  TeV is a pivotal factor to distinguish between the hadronic or leptonic origin of the  $\gamma$ -ray emission and to constrain the acceleration mechanism. The MAGIC telescopes resolved for the first time this TeV region, finding that  $E > 10$  TeV emission comes only from the tail region, where the SNR G106.3+2.7 resides. However, additional and more precise measurements are required to confirm these results.

In this context, the ASTRI Mini-Array can play a crucial role. Thanks to its performance in the multi-TeV band, this facility will make an essential contribution to understanding the nature of the UHE emission shedding light on its possible relation with CR origin.

Building on the latest important results reported by the MAGIC collaboration, this work aims at investigating the potential of ASTRI-MiniArray in studying the complex morphology of this source and showing the potential improvements which can be obtained thanks to deep observation of the source.

38th International Cosmic Ray Conference (ICRC2023)  
26 July - 3 August, 2023  
Nagoya, Japan



\*<http://www.astri.inaf.it/en/library/>

\*Speaker

## 1. Introduction

Despite the enormous efforts done in recent years, the primary three questions about the Cosmic Ray (CR) origin still need to be clarified: what are their sources, how are they accelerated, and how do they propagate?

Gamma-ray astronomy plays a fundamental role in this field. Both relativistic protons and electrons can emit in the  $\gamma$ -ray band through different processes, but only the detection of hadronic  $\gamma$ -ray emission can probe CR acceleration. The recent detection of several PeV Galactic sources by the LHAASO collaboration [3] represents a breakthrough in Cosmic Ray (CR) origin search. On one side, most of these sources are likely leptonic accelerators, showing that a  $\gamma$ -ray detection at PeV energies cannot by itself be considered the final proof of hadronic acceleration (i.e. CR acceleration). On the other, it confirms that there is a real possibility that sources other than Supernova Remnants (SNRs) could accelerate Galactic CRs. Furthermore, the limited angular resolution of LHAASO (about  $0.3^\circ$  at 100 TeV) makes associations uncertain, and more detailed studies are needed. All the 12 LHAASO PeVatrons (but the Crab Nebula) have several possible TeV counterparts that could be associated with the unresolved LHAASO  $\gamma$ -ray emission [3] and several kinds of sources could be at the origin of this emission, from Pulsar Wind Nebule (PWNe) to SNRs to Young Massive Star Clusters (YMSCs) to TeV halos [see 4, for a recent review].

In this context, the ASTRI Mini-Array [14, 17, 10, 16], nine small-size Cherenkov Telescopes that are being built at the Teide Observatory in Tenerife, can play a fundamental role. The first three telescopes will be operative by the beginning of 2024, and the full array within a few years. With its unprecedented sensitivity among existing Imaging Atmospheric Cherenkov Telescopes (IACTs) in the multi-TeV band and high angular resolution ( $0.05^\circ$  at 100 TeV) [12], the ASTRI Mini-Array, with deep observations ( $> 100$  hrs per source), can explore the  $\gamma$ -ray spectra of candidate PeVatrons and resolve their morphology, shedding light on the nature of the highest energy emission.

In this work, we focus on one of the LHAASO candidate PeVatrons, LHAASO J2226+6057, detected with a very high significance at  $E > 100$  TeV ( $13.6\sigma$ ) and for which a SED at UHE was extracted, with a maximum energy  $E_M \approx 570$  TeV. Its TeV counterparts are VER J2227+608/HAWC J2227+610 [20], and two sources could explain this VHE/UHE emission: the SNR G106.3+2.7 with the associated Molecular Cloud (MC) located in the “tail” of the VHE emission, and the Boomerang PWN, associated with the PSR J2229+6141 in the “head”. Identifying the exact origin of the emission at 100 TeV (and above) is a key factor in distinguishing between a hadronic or leptonic origin of the UHE emission and in understanding the particle acceleration mechanisms.

This region was already detected at UHE by HAWC [2], Tibet AS $\gamma$  [18], and finally by LHAASO [3] but we were not able to say if UHE  $\gamma$ -ray originate from the head or the tail region. A 12-year Fermi-LAT GeV data analysis of the region showed that at the highest energies (10–500 GeV), only the tail is emitting  $\gamma$ -ray and recently, the MAGIC telescopes resolved for the first time this region at TeV energies, finding that  $E > 10$  TeV emission comes only from the tail region, where the SNR G106.3+2.7 resides [13]. However, additional and more precise measurements are required to confirm these results.

The real origin of the TeV emission will only be understood with a deep analysis of the microphysics of the region but, regardless of a PWN or SNR origin, a hadronic origin is largely favoured [21, 11] and supported also by the analysis of non-thermal X-ray radiation [21, 9, 8,

11], detected everywhere but with an enhancement of the luminosity in the head region, and well correlated with the radio emission but not with the  $\gamma$ -ray emission.

In this context, the ASTRI Mini-Array can play a crucial role. With its unprecedented sensitivity and, in particular, angular resolution in the multi-TeV band compared to existing IACTs, this facility will make an important contribution to understanding the nature of the UHE emission shedding light on its possible relation with CRs. Before the last LHAASO results, a first simulation of the ASTRI Mini-Array performance on this source was done for the ASTRI Mini-Array Core Science paper [19]. There it is shown how the ASTRI Mini-Array will be able to detect this source up to (and above) 100 TeV with a high significance and strong constraints on the cut-off energy. After the LHAASO results, we decided to focus our efforts on the fundamental morphological analysis of the LHAASO J2226+6057. Taking advantage of the latest important results reported by the MAGIC collaboration, this work aims to investigate the potential of the ASTRI Mini-Array in studying this complex source morphology and in showing the potential improvements which can be obtained thanks to deep observations of the source.

In Section 2 we present the set-up of our simulations and analysis, showing the obtained results in Section 3 from a spatial (Section 3.1) and spectral (Section 3.2) point of views. Our conclusions are presented in Section 4.

## 2. Simulations and analysis

To perform both data simulation and analysis of the source, we used *Gammapy* v1.0 [6].

The source is simulated in a  $3^\circ \times 3^\circ$  field of view, centred on the position of SNR G106.3+2.7 ( $R.A. = 336.875^\circ$ ,  $Dec = 60.833^\circ$ ), with a spatial bin size of  $0.02^\circ$ . The emission is studied in an energy range 1 – 300 TeV, divided into 20 energy bins. For simulation and analysis, we used the ASTRI Mini-Array Instrument Response Function (IRF) [15]. The IRF includes the effective area, the angular and energy resolution, and the background rate due to CRs mis-reconstructed as  $\gamma$ -ray photons. From the ASTRI Mini-Array site (Observatorio del Teide, in the Canarian Island Tenerife), the SNR G106.3+2.7 is observable at zenith angle  $< 45^\circ$  for about 450 hours per year in moonless conditions. Consequently, we considered a realistic exposure time of 200 hours. To reduce the impact of random variations between individual realizations, we performed a set of  $N = 100$  statistically independent simulations. We then fitted each of the 100 simulated data with a maximum likelihood analysis adopting the same model and averaged the results, in order to statistically characterize the morphological and spectral features of the observed source.

Following the MAGIC collaboration work [13], we performed our simulations with the assumption that the  $\gamma$ -ray emission from this source has a complex energy-dependent origin, with the emission at  $E > 10$  TeV coming mainly from the “tail” region. Consequently, we simulated the source using two different components, one for the “head” and one for the “tail”, modelling both with a Symmetrical Gaussian (i.e. a circle with a Gaussian profile) spatial distribution. From a spectral point of view, we modelled the two components based on the model built by MAGIC [13] on the analysis of multi-wavelength data. On one hand, we assume that the observed  $\gamma$ -ray radiation from the “head” region is mainly produced by Inverse Compton (IC) scattering from an electron power law distribution with spectral index 2.6, exponential cutoff at 360 TeV and total energy  $> 1$  GeV of  $W_e = 1.4 \times 10^{47}$  erg. On the other hand, for the “tail” region we assumed the presence

of a population of leptons and a larger contribution from hadrons interacting with MCs near the source via the pion decay channel. Both particle populations are described by a power law with, respectively, spectral index 2.5 and 1.7, exponential cutoff at 35 TeV and 1000 TeV, total energy  $> 1$  GeV of  $W_e = 2 \times 10^{46}$  erg and  $W_p = 8.2 \times 10^{45}$  erg.

We computed non-thermal radiation from relativistic particle populations using the package *naima* [22], assuming a source distance of 800 pc and a target density of  $200 \text{ cm}^{-3}$  [13] (see Figure 3).

We performed our analysis on a 3D binned dataset: two axes for longitude and latitude coordinates and the third axis for energy. For modelling and fitting, the simulated events files are reduced by binning the events into a counts map and interpolating exposure, background, PSF and energy dispersion on the chosen analysis geometry. The fit is performed using the *minuit* backend [7] with default parameters. Our test hypothesis is based on the *cstat* statistics [5], where the fit improvement is quantified by  $TS = 2 \times (\log \mathcal{L}_0 - \log \mathcal{L}_{mod})$  for the maximum likelihood of a generic model ( $\mathcal{L}_{mod}$ ) compared to our null hypothesis ( $\mathcal{L}_0$ ).

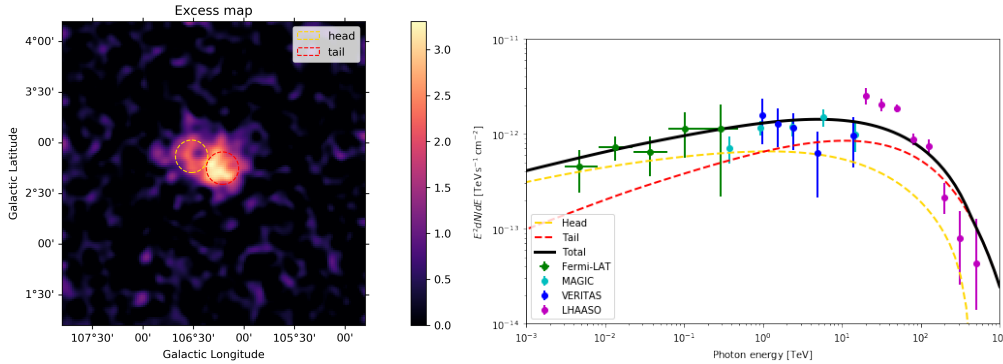


**Figure 1:** *Left:* simulated excess map for 200 hours of observation of the SNR G106.3+2.7. The map is smoothed with a  $0.05^\circ$  Gaussian  $\sigma$  corresponding to the ASTRI Mini-Array angular resolution at 10 TeV. The yellow (red) circle shows the simulated spatial region for the “head” (“tail”) region. *Right:* template spectral energy distribution used for modelling the source. Dashed lines represent the contributions of the “head” and “tail” areas, while the continuous line indicates the total contribution (obtained as the sum of the two contributions). Green, cyan, blue and magenta dots show the *Fermi*-LAT [21], MAGIC [13], VERITAS [1] and LHAASO [3] measurements, respectively.

### 3. Results

#### 3.1 Morphological Analysis

As a first step in our analysis, we performed a morphological investigation in the entire energy range to better understand the ASTRI Mini-Array capability to characterise the spatial properties of the source. To fit the data cubes, we tested the following spatial models: a point source, a Symmetric Disk (i.e. a circle with a constant profile), a Symmetric Gaussian, an Elliptical Disk and an Elliptical Gaussian (that is, respectively, an ellipse with a constant profile and one with a Gaussian profile), and our original model consisted of two Symmetrical Gaussian. Our null hypothesis is the model without emission from the source, which has a maximum likelihood  $\mathcal{L}_0$ . For all tested

**Table 1:** Average best-fit test statistics of the G106.3+2.7 for different morphological models compared with the null hypothesis of no  $\gamma$ -ray emission from the SNR (1 – 250 TeV).

| Model                 | TS  | Additional DoF |
|-----------------------|-----|----------------|
| PointSource           | 107 | 2              |
| Symmetric Disk        | 597 | 3              |
| Symmetric Gaussian    | 645 | 3              |
| Elliptical Disk A     | 614 | 4              |
| Elliptical Disk B     | 619 | 4              |
| Elliptical Gaussian A | 647 | 4              |
| Elliptical Gaussian B | 666 | 4              |
| Elliptical Disk C     | 642 | 5              |
| Elliptical Gaussian C | 673 | 5              |
| Original model        | 671 | 6              |

spatial models, we assumed a power law spectral model with all free parameters. For the Elliptical Disk and Gaussian, we assumed three different parameterizations: A) fixed eccentricity value at 0.60 and a free rotation angle  $\phi$  (increasing counter-clockwise from the North direction); B) free eccentricity and a fixed  $\phi$  at  $55^\circ$ ; C) both variable eccentricity and  $\phi$ . For the original model used in the simulations, we kept the central positions of the two disks fixed, keeping variable only their radius.

The obtained results are shown in Table 1. If compared to the Gaussian or Disk models, the point source hypothesis is clearly excluded with a  $> 5\sigma$  confidence level, implying a clear detection of the extension of the source. Although the original model achieves the highest TS values, these values are not significantly higher than those obtained for a morphology described by an Elliptical Gaussian B or C. Consequently, it is not possible to identify a significant difference between the “head” and “tail” regions through an analysis of the entire energy band. For this reason, we performed different fits in different energy ranges (1 – 10, 10 – 50 and 50 – 250 TeV) in order to test the capability of detecting an energy-dependent morphology. We used a Symmetrical Gaussian function as a spatial model and a power law as a spectral model. From the fits, it emerged that the central position of the peak  $\gamma$ -ray emission tends to move towards the “tail” region with increasing energy. On the other hand, the lower energy emission extends close to the “head” position, as shown in Figure 2. These results are in agreement with the MAGIC ones that show the highest energy emission focused on the “tail” region.

### 3.2 Spectral Analysis

The next step was the analysis of the emission spectrum of the source, testing several models: a power law, a power law with an exponential cutoff and a LogParabola. We assumed the Elliptical Gaussian B spatial model for all spectral models tested. A simple power law fits the data quite well, while the addition of a cut-off or a curved spectrum leads to an improvement of slightly less than  $3\sigma$  with respect to the power law model (see Table 2). Motivated by the morphological analysis that suggests an energy dependence in the spatial emission, we decided to study the emission spectrum separately in the “head” and “tail” regions. To do this, the spectral study is performed

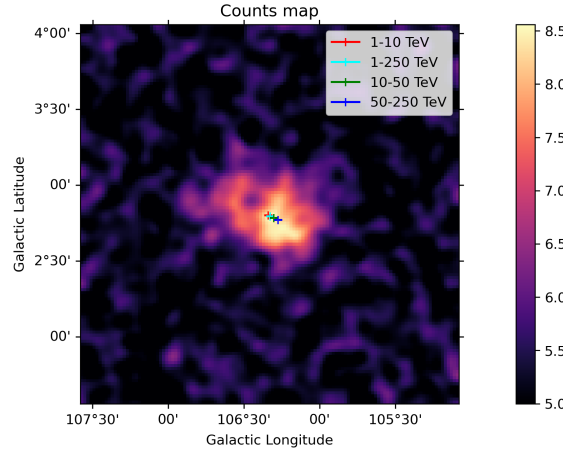


**Figure 2:** Simulated counts map for 200 hours of observation of the SNR G106.3+2.7. The map is smoothed with a  $0.05^\circ$  Gaussian  $\sigma$ . The cross symbols show the best-fit position of symmetric Gaussian in different energy bands.

**Table 2:** Best-fit test statistics of the G106.3+2.7 for different spectral models compared with the null hypothesis of a power law  $\gamma$ -ray emission associated with the SNR (1 – 250 TeV).

| Model             | Spectral Model   | TS | Additional DoF |
|-------------------|--|----|----------------|
| PowerLaw          | $N_0 \cdot \left(\frac{E}{E_0}\right)^{-\gamma}$                                     | 0  | 0              |
| ExponentialCutoff | $N_0 \cdot \left(\frac{E}{E_0}\right)^{-\gamma} \exp\left(-\frac{E}{E_{cut}}\right)$ | 6  | 1              |
| LogParabola       | $N_0 \cdot \left(\frac{E}{E_0}\right)^{-\alpha-\beta \log(E/E_0)}$                   | 5  | 2              |

using the original model used for morphological simulations of the two regions. We performed a fit on the data using different combinations of the spectral models mentioned above on both regions simultaneously. As shown in Table 3, a combination of a power law model for the “head” region and an exponential cutoff, with a cut-off in the  $\gamma$ -ray energy emission of  $91 \pm 6$  TeV, for the “tail” region is preferred. Even if there is no evident cut-off in the best-fit model for the “head” emission, it is subdominant with respect to the “tail” one, in particular at the highest energies. A  $\gamma$ -ray cut-off at about 90 TeV implies a hadronic cut-off at about 1 PeV, pointing one more time toward the possibility that the SNR G106.3+2.7 could be a CR accelerator. However, in spite of the theoretical interpretation of these results, it is clear that ASTRI Mini-Array will be able to characterize the spectra from the two different regions of the SNR G106.3+2.7 (and similar sources).

#### 4. Conclusions

In this work, we have shown the possible perspectives and potential for the ASTRI Mini-Array in the study of the morphology of the PeVatron SNR G106.3+2.7, recently observed by several facilities at energies  $> 100$  TeV. Using the python library `gammapy`, we simulated 200 hours of source observation with the ASTRI Mini-Array, exploiting recent results from the MAGIC collaboration. We assumed that the source emission came from two main regions, the “head” and



**Table 3:** Best-fit test statistics for different spectral models compared with the null hypothesis of a power law  $\gamma$ -ray emission in the “head” and “tail” regions.

| Head              | Tail              | TS | Additional DoF |
|-------------------|-------------------|----|----------------|
| PowerLaw          | PowerLaw          | 0  | 0              |
| ExponentialCutoff | PowerLaw          | 10 | 1              |
| PowerLaw          | ExponentialCutoff | 11 | 1              |
| ExponentialCutoff | ExponentialCutoff | 7  | 2              |
| LogParabola       | PowerLaw          | 9  | 2              |
| PowerLaw          | LogParabola       | 10 | 2              |
| ExponentialCutoff | LogParabola       | 13 | 3              |
| LogParabola       | ExponentialCutoff | 14 | 3              |
| LogParabola       | LogParabola       | 14 | 4              |

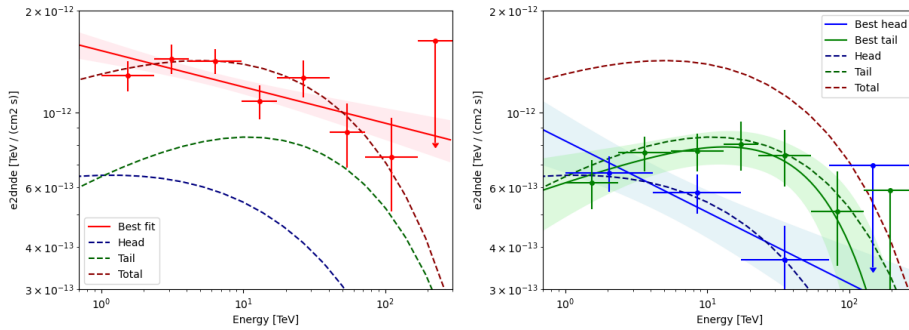


**Figure 3:** Flux points of the SNR G106.3+2.7 as seen by ASTRI Mini-Array with 200 hours of observation. Dashed blue and green lines represent the contributions of the “head” and “tail” areas to the template spectral energy distribution used for modelling the source, while the red dashed line indicates the total contribution (obtained as the sum of the two contributions). *Left:* the flux points are obtained assuming the best-fitted model for the entire SNR which is shown as a solid red line. *Right:* the flux points are extracted from the “head” (blue) and “tail” (green) regions separately, best-fit spectral models are shown as solid lines.

the “tail”, the former of leptonic origin and the latter due mainly to hadrons. Our morphological analysis reveals how well ASTRI Mini-Array can characterise the extended source emission up to 300 TeV. Moreover, it shows how the Mini-Array will be able to confirm the energy-dependent nature of the morphology, by detecting the emission peak at low energies towards the “head” region and that at higher energies towards the “tail”. The spectral analysis, instead, showed that the ASTRI Mini-Array, with a 200-hour exposure, will be able to reveal spectral differences in different regions of the source, providing an important tool for understanding the different nature of PeVatronic emission in the source.

## Acknowledgments

This work was conducted in the context of the ASTRI Project. We gratefully acknowledge support from the people, agencies, and organisations listed here: <http://www.astrif.inaf.it/en/library/>. This paper went through the internal ASTRI review process.

## References

- [1] V. A. Acciari et al. “Detection of Extended VHE Gamma Ray Emission from G106.3+2.7 with Veritas”. In: *The Astrophysical Journal Letters* 703.1 (Sept. 2009), pp. L6–L9. doi: 10.1088/0004-637X/703/1/L6. arXiv: 0911.4695 [astro-ph.HE].
- [2] A. Albert et al. “HAWC J2227+610 and Its Association with G106.3+2.7, a New Potential Galactic PeVatron”. In: *The Astrophysical Journal Letters* 896.2, L29 (June 2020), p. L29. doi: 10.3847/2041-8213/ab96cc. arXiv: 2005.13699 [astro-ph.HE].
- [3] Zhen Cao et al. “Ultrahigh-energy photons up to 1.4 petaelectronvolts from 12  $\gamma$ -ray Galactic sources”. In: *Nature* 594.7861 (June 2021), pp. 33–36. doi: 10.1038/s41586-021-03498-z.
- [4] Martina Cardillo and Andrea Giuliani. “The LHAASO PeVatron bright sky: What we learned”. en. In: *Appl. Sci. (Basel)* 13.11 (May 2023), p. 6433.
- [5] W. Cash. “Parameter estimation in astronomy through application of the likelihood ratio.” In: *The Astrophysical Journal* 228 (Mar. 1979), pp. 939–947. doi: 10.1086/156922.
- [6] C. Deil et al. “Gammapy - A prototype for the CTA science tools”. In: *35th International Cosmic Ray Conference (ICRC2017)*. Vol. 301. International Cosmic Ray Conference. July 2017, 766, p. 766. doi: 10.22323/1.301.0766. arXiv: 1709.01751 [astro-ph.IM].
- [7] Hans Dembinski and Piti Ongmongkolkul et al. “scikit-hep/iminuit”. In: (Dec. 2020). doi: 10.5281/zenodo.3949207. URL: <https://doi.org/10.5281/zenodo.3949207>.
- [8] Yutaka Fujita et al. “X-Ray Emission from the PeVatron-candidate Supernova Remnant G106.3+2.7”. In: *The Astrophysical Journal* 912.2, 133 (May 2021), p. 133. doi: 10.3847/1538-4357/abf14a. arXiv: 2101.10329 [astro-ph.HE].
- [9] Chong Ge et al. “Revealing a peculiar supernova remnant G106.3+2.7 as a petaelectronvolt proton accelerator with X-ray observations”. In: *The Innovation* 2, 100118 (May 2021), p. 100118. doi: 10.1016/j.xinn.2021.100118. arXiv: 2012.11531 [astro-ph.HE].
- [10] Enrico Giro et al. “The ASTRI-Horn telescope validation toward the production of the ASTRI Mini-Array: a proposed pathfinder for the Cherenkov Telescope Array”. In: *Optics for EUV, X-Ray, and Gamma-Ray Astronomy IX*. Ed. by Stephen L. O’Dell and Giovanni Pareschi. Vol. 11119. Society of Photo-Optical Instrumentation Engineers (SPIE) Conference Series. Sept. 2019, 111191E, 111191E. doi: 10.1117/12.2530896.
- [11] Xuan-Han Liang et al. “A PeVatron Candidate: Modeling the Boomerang Nebula in X-ray Band”. In: *Universe* 8.10 (Oct. 2022), p. 547. doi: 10.3390/universe8100547. arXiv: 2209.03809 [astro-ph.HE].
- [12] S. Lombardi et al. “Performance of the ASTRI Mini-Array at the Observatorio del Teide”. In: *37th International Cosmic Ray Conference*. Mar. 2022, 884, p. 884. doi: 10.22323/1.395.0884.
- [13] MAGIC Collaboration et al. “MAGIC observations provide compelling evidence of hadronic multi-TeV emission from the putative PeVatron SNR G106.3+2.7”. In: *Astronomy and Astrophysics* 671, A12 (Mar. 2023), A12. doi: 10.1051/0004-6361/202244931. arXiv: 2211.15321 [astro-ph.HE].
- [14] G. Pareschi et al. “The Dual-mirror Small Size Telescope for the Cherenkov Telescope Array”. In: *International Cosmic Ray Conference*. Vol. 33. International Cosmic Ray Conference. Jan. 2013, p. 1151. doi: 10.48550/arXiv.1307.4962. arXiv: 1307.4962 [astro-ph.IM].
- [15] ASTRI Project. *ASTRI Mini-Array Instrument Response Functions (Prod2, v1.0)*. Version 1.0. <http://www.astri.inaf.it/en/library/>. Zenodo, July 2022. doi: 10.5281/zenodo.6827882. URL: <https://doi.org/10.5281/zenodo.6827882>.
- [16] S. Scuderi et al. “The ASTRI Mini-Array of Cherenkov telescopes at the Observatorio del Teide”. In: *Journal of High Energy Astrophysics* 35 (Aug. 2022), pp. 52–68. doi: 10.1016/j.jheap.2022.05.001. arXiv: 2208.04571 [astro-ph.IM].
- [17] Salvatore Scuderi. “The ASTRI Program”. In: *European Physical Journal Web of Conferences*. Vol. 209. European Physical Journal Web of Conferences. Sept. 2019, 01001, p. 01001. doi: 10.1051/epjconf/201920901001.
- [18] Tibet AS $\gamma$  Collaboration et al. “Potential PeVatron supernova remnant G106.3+2.7 seen in the highest-energy gamma rays”. In: *Nature Astronomy* 5 (Jan. 2021), pp. 460–464. doi: 10.1038/s41550-020-01294-9. arXiv: 2109.02898 [astro-ph.HE].
- [19] S. Vercellone et al. “ASTRI Mini-Array core science at the Observatorio del Teide”. In: *Journal of High Energy Astrophysics* 35 (Aug. 2022), pp. 1–42. doi: 10.1016/j.jheap.2022.05.005. arXiv: 2208.03177 [astro-ph.HE].
- [20] S. P. Wakely and D. Horan. “TeVcat: An online catalog for Very High Energy Gamma-Ray Astronomy”. In: *International Cosmic Ray Conference*. Vol. 3. International Cosmic Ray Conference. Jan. 2008, pp. 1341–1344.
- [21] Yuliang Xin et al. “VER J2227+608: A Hadronic PeVatron Pulsar Wind Nebula?” In: *The Astrophysical Journal* 885.2, 162 (Nov. 2019), p. 162. doi: 10.3847/1538-4357/ab48ee. arXiv: 1907.04972 [astro-ph.HE].
- [22] V. Zabalza. “naima: a Python package for inference of relativistic particle energy distributions from observed nonthermal spectra”. In: *Proc. of International Cosmic Ray Conference 2015* (2015), p. 922. eprint: 1509.03319.